Analysis Of An Ac-Dc Full-Controlled Converter Supplying Dc Series Motor Parallel With An Inductive R-L Load

Mohammed M. Al-Hindawi , Yusuf A Al-Turki

Department of Electrical and Computer Engineering, King Abdulaziz University, Jeddah, Saudi Arabia
mar7636@hotmail.com

Abstract: This paper is concerned with the detailed study of performance characteristics of an ac-dc full-controlled converter supplying dc series motor parallel with an inductive R-L load. The converter-loads combination is simulated on a digital computer. Different modes of operation (continuous and discontinuous converter currents) are considered. A formula is derived for the critical firing angle. Different performance parameters are studied for both constant motor horsepower level and constant firing angle. The effects of variation of the passive load phase angle and impedance have been studied. In order to verify the accuracy and validity of the analysis presented, the converter-loads combination has been assembled and investigated experimentally.

[Al-Hindawi M, Al-Turki Y. **Analysis Of An Ac-Dc Full-Controlled Converter Supplying Dc Series Motor Parallel With An Inductive R-L Load.** *Life Sci J* 2014;11(9):78-92]. (ISSN:1097-8135). http://www.lifesciencesite.com. 12

Keywords: Controlled rectifiers; AC-DC converters; Full-controlled converters; Series-motor parallel with an inductive R-L load.

1. Introduction

In recent years, the DC series motor drives are engaged with wide range of applications. The application of DC series motor in industrial environment has increased due to high performance and high starting torque as suitable drive system (Masilamani Muruganadam and Muthusamy Madheswaran, 2013) and (Muruganadam M and Madheswaran M, 2012). In phase controlled converters, thyristor commutation is easily achieved by the naturel or line commutation. No additional circuitry is requred for the commutation process. Phase controlled converters are simple, less expensive and are extensively used in industries (Hart D H ,2011), (Rashed M H,2004) ,(Singh M D, 2003) and (Sen P C, 1981). Most of the work reported in the literature is related to AC-DC converter supplying a dc motor (Sen P C,1981) , (Sen P C and Dorodla S R, 1975) and (Sen P C, 1990) or two-parallel passive loads (Yung- Chung Li,1978) and (Al-Johani A H,1987) or two motor loads (Al-Subaie,1999) , (Al-Turki Y A, Al-Hindawi M M and Al Subaie O T,2001) and (Al-Hindawi M M, Al-Turki Y A and Al Subaie O T,2000). The analysis of full-converter supplying separately excited DC motor parallel with an inductive R-L load and the analysis of semi converter supplying series motor parallel with the same inductive R-L load is reported in (Al-Turki Y, Al-Hindawi M M and Al-Sobaie O T,2000) and (Al-Hindawi M M, Al-Turki Y A and Maghrabi M,2006). The presence of full-controlled converter supplying DC series motor connected in parallel with an inductive R-L load is commonly found in practice. The analysis and performance parameters reported in the literature for an AC-DC converters cannot be applied in such a situation.

In this paper, analysis of a phase-controlled (AC-DC full-controlled) converter feeding a series dc motor parallel with an inductive R-L load will be investigated. The steady-state analysis of this system will be obtained for each of the two modes of operation, i.e. continuous and discontinuous converter current. An expression for the critical firing angle at which the converter current changes from one mode to the other will be deduced. Performance parameters such as, input power factor, supply current distortion factor, torque-speed characteristics, and motor current ripple factor have been derived and studied for both constant firing angle and constant motor horsepower level. The effects of variation of the passive load phase angle and impedance have been studied. The theoretical and experimental results are compared to check model effectiveness.

2. Steady state analysis

Figure 1 shows an AC-DC full-controlled converter supplying dc series motor parallel with an inductive R-L load. The sinusoidal voltage source is considered to have an rms value of V volts, frequency of $\omega/2\pi$ Hz and zero internal impedance. Changing the thyristors firing-angles controls the load voltage and currents. The converter current may be continuous or discontinuous depending on the value of the firing angles, the load parameters, and the motor speed. Thyristors S1 and S3 are fired at an angle α relative to the supply zero voltage whereas S2 and S4 are gated at $\pi+\alpha$. Each of the two modes of operation will be treated separately.

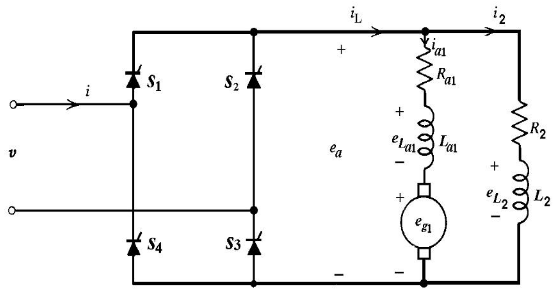

Figure 1. Full controlled converter supplying dc series motor parallel with an inductive R-L load

2.1 Continuous Mode:

The converter current il in this mode has a positive value throughout the period of α≤ωt≤π+α. The load voltage across each branch is equal to the supply voltage assuming zero drop across each thyristor. This means that: for the dc series motor,

$$\sqrt{2}V\sin\omega t = i_{c1}R_{a1} + L_{a1}\frac{d}{dt}i_{c1} + K_{af}i_{c1}N + K_{res}N \quad (1)$$

and for the passive load,

$$\sqrt{2}V\sin\omega t = i_{c2}R_2 + L_2\frac{d}{dt}i_{c2} \quad (2)$$

Where: ic1 is the armature current (ia1) and ic2 is the passive load current during the continuous mode.

During this mode, the converter current i_{cl} equals the supply current i_{cs} and is given by:

$$i_{cs} = i_{cl} = i_{c1} + i_{c2},\ \alpha \le \omega t \le \pi+\alpha \quad (3)$$

If steady-state speed and magnetic linearity are assumed, the solution of equation (1) is of the form:

$$i_{c1} = \sqrt{2}(V/Z_1)\sin(\omega t - \phi_1) + K_{c1}e^{(-(\omega t-\alpha)/Q_1)} - (K_{res}N/R_1)(1 - e^{(-(\omega t-\alpha)/Q_1)}) \quad (4)$$

Where: $R_1 = R_{a1} + K_{af}N$, K_{af} and K_{res} are constants.

Full expressions for the average and rms values of the motor current (I_{c1av} and I_{c1rms}) are given in the appendix and the ripple factor of ic1 is given by:

$$K_{cr1} = \sqrt{I_{c1rms}^2 / I_{c1av}^2 - 1} \quad (6)$$

The solution of equation (2) is:

$$i_{c2} = \sqrt{2}(V/Z_2)\sin(\omega t - \phi_2) + K_{c2}e^{(-(\omega t-\alpha)/Q_2)} \quad (7)$$

Where: $Z_2 = \sqrt{R_2^2 + (\omega L_2)^2}$, $Q_2 = \omega L_2 / R_2$,

$\phi_2 = \tan^{-1}(\omega L_2 / R_2)$,

$K_{c2} = I_{c2} - \sqrt{2}(V/Z_2)\sin(\alpha - \phi_2)$, and Ic2 is the initial value of ic2 at ωt = α .

Under steady state operation, ic2 at ωt = α equals that at ωt= π+α and is equal to:

$$I_{c2} = -\sqrt{2}(V/Z_2)[(1 + e^{(-\pi/Q_2)})/(1 - e^{(-\pi/Q_2)})]\sin(\alpha - \phi_2) \quad (8)$$

Full expressions for the average and rms value of the passive load current (I_{c2av} and I_{c2rms}) are given in the appendix and the rms value of the supply current is obtained as:

$$I_{csrms} = \sqrt{(1/\pi)\int_{\alpha}^{\pi+\alpha} i_{cs}^2\, d\omega t} = \sqrt{I_{c1rms}^2 + I_{c2rms}^2 + (1/\pi)\int_{\alpha}^{\pi+\alpha} 2 i_{c1} i_{c2}\, d\omega t} \quad (9)$$

The rms value of the fundamental component of the supply current is:

$$I_{cf} = \sqrt{\left(a_{c1}^2 + b_{c1}^2\right)/2} \quad (10)$$

Full expressions for the rms value of the supply current (I_{csrms}) and the amplitudes of the cosine and sine fundamental components (ac1 and bc1) of the same current are given in the appendix and the phase angle of that component is given by: $\theta = \tan^{-1}(a_{c1}/b_{c1})$ (11)

The supply power factor is:

$$Pf = (I_{cf} / I_{csrms})\cos\theta \quad (12)$$

Whereas the supply current distortion factor is:

$$Df = I_{cf} / I_{csrms} \quad (13)$$

The critical firing angle αc, which is the highest firing angle for the continuous mode, satisfies the condition of: $I_{c1} + I_{c2} = 0$ (14)

Therefore, the critical firing angle αc is given from:

$$\alpha_c = \sin^{-1}[(A_1C_1 \pm \sqrt{A_1^2C_1^2 + (A_1^2 + B_1^2)(B_1^2 - C_1^2)})/(A_1^2 + B_1^2)] \quad (15)$$

Where: $A_1 = F_1\cos\phi_1 + F_2\cos\phi_2$,

$F_1 = -(\sqrt{2}V/Z_1)(1 + e^{(-\pi/Q_1)})/(1 - e^{(-\pi/Q_1)})$,

$F_2 = -(\sqrt{2}V/Z_2)(1 + e^{(-\pi/Q_2)})/(1 - e^{(-\pi/Q_2)})$,

$B_1 = F_1\sin\phi_1 + F_2\sin\phi_2$, and $C_1 = K_{res}N/R_1$.

If K_{res} has a negligible value, α_c is independent of the supply voltage.

When ϕ1 =ϕ2 =ϕ then α_c=ϕ, ignoring the effect of K_{res}.

2.2 Discontinuous Mode

In this mode, α>αc and the current idl increases from zero at ωt=α to a maximum value and then decreases to become zero again at ωt=β which is referred to as the extinction angle. The angle β is, of course, less-than π+α.

Throughout the period α≤ωt≤β, the load voltage equals the supply voltage. This means that:

for the motor,

$$\sqrt{2}V\sin\omega t = i_{d1}R_{a1} + L_{a1}\frac{d}{dt}i_{d1} + K_{af}i_{d1}N + K_{res}N \quad (16)$$

and for the passive load,

$$\sqrt{2}V\sin\omega t = i_{d2}R_2 + L_2\frac{d}{dt}i_{d2} \quad (17)$$

During α≤ωt≤β, the converter current idl equals the supply current and is given by:

$$i_{ds} = i_{dl} = i_{d1} + i_{d2}$$

The solution of equation (16) is of the form:

$$i_{d1} = \sqrt{2}(V/Z_1)\sin(\omega t - \phi_1) + K_{d1}e^{(-(\omega t-\alpha)/Q_1)} - (K_{res}N/R_1)(1 - e^{(-(\omega t-\alpha)/Q_1)}) \quad (19)$$

Where: $K_{d1} = \mathrm{I}_{d1} - (\sqrt{2}V/Z_1)\sin(\alpha - \phi_1)$ (20)

and Id1 is the initial value of id1 at ωt=α.

The solution of equation (17) is of the form:

$$i_{d2} = \sqrt{2}(V/Z_2)\sin(\omega t - \phi_2) + K_{d2}e^{(-(\omega t-\alpha)/Q_2)} \quad (21)$$

Where: $K_{d2} = \mathrm{I}_{d2} - (\sqrt{2}V/Z_2)\sin(\alpha - \phi_2)$ (22)

and Id2 is the initial value of id2 at ωt=α.

During the period β≤ωt≤π+α, the converter current is equal to zero, and $i_{d1} = -i_{d2}$.

During this period the motor and the passive load are connected in parallel. Thus:

$$R_1 i_{d1} + L_{a1}\frac{d}{dt}i_{d1} + K_{res}N = R_2 i_{d2} + L_2\frac{d}{dt}i_{d2} \quad (23)$$

Solving (23), one obtains:

$$i_{d1} = (-K_{res}N)/(R_1 + R_2) + (I'_{d1} + K_{res}N/(R_1 + R_2))e^{(-(\omega t-\beta)/Q)} \quad (24)$$

Similarly:

$$i_{d2} = (K_{res}N)/(R_1 + R_2) + (I'_{d2} - K_{res}N/(R_1 + R_2))e^{(-(\omega t-\beta)/Q)} \quad (25)$$

Where: $Q = \omega(L_{a1} + L_2)/(R_1 + R_2)$,

I'_{d1} is the initial value of id1 at ωt=β and is given by:

$$I'_{d1} = (\sqrt{2}V/Z_1)\sin(\beta - \phi_1) + K_{d1}e^{(-(\beta-\alpha)/Q_1)} - (K_{res}N/R_1)(1 - e^{(-(\beta-\alpha)/Q_1)}) \quad (26)$$

and I'_{d2} is the initial value of id2 at ωt=β and is given by:

$$I'_{d2} = (\sqrt{2}V/Z_2)\sin(\beta - \phi_2) + K_{d2}e^{(-(\beta-\alpha)/Q_2)} \quad (27)$$

At ωt=π+α, id1 equals Id1, and id2 equals Id2 Therefore, from equations (20), (24), and (26) one gets:

$$I_{d1} = [((-K_{res}N)/(R_1 + R_2))(1 - e^{(-(\pi+\alpha-\beta)/Q)}) + (\sqrt{2}V/Z_1)(\sin(\beta - \phi_1) - \sin(\alpha - \phi_1)e^{(-(\beta-\alpha)/Q_1)})e^{(-(\pi+\alpha-\beta)/Q)} - (K_{res}N/R_1)(1 - e^{(-(\beta-\alpha)/Q_1)})e^{(-(\pi+\alpha-\beta)/Q)}]/(1 - e^{(-(\beta-\alpha)/Q_1)}e^{(-(\pi+\alpha-\beta)/Q)}) \quad (28)$$

(18)

Similarly: from equations (22), (25), and (27) one gets:

$$I_{d2} = [((K_{res}N)/(R_1 + R_2))(1 - e^{(-(\pi+\alpha-\beta)/Q)}) + (\sqrt{2}V/Z_2)(\sin(\beta - \phi_2) - \sin(\alpha - \phi_2)e^{(-(\beta-\alpha)/Q_2)})e^{(-(\pi+\alpha-\beta)/Q)}]/(1 - e^{(-(\beta-\alpha)/Q_1)}e^{(-(\pi+\alpha-\beta)/Q)}) \quad (29)$$

The extinction angle β is determined by the solution of the equation Id1=-Id2. (30)

Full expressions for I_{d1av}, I_{d1rms}, I_{d2av}, I_{d2rms}, and I_{dsrms} are given in the appendix. Where: I_{d1av} ,and I_{d1rms} are the average and rms values of the motor current respectively.

I_{d2av} ,and I_{d2rms} are the average and rms values of the passive load current respectively, and I_{dsrms} is the rms value of the supply current.

The ripple factor of i_{d1} will be given by:

$$K_{dr1} = \sqrt{(I_{d1rms}^2 / I_{d1av}^2) - 1} \quad (31)$$

The rms value of the fundamental component of the supply current is: $I_{df} = \sqrt{(a_{d1}^2 + b_{d1}^2)/2}$ (32)

Where: ad1 and bd1 are the amplitudes of the cosine and sine fundamental components of ids respectively and their full expressions are given in the appendix. phase angle of the fundamental component of the supply current is given by: $\theta = \tan^{-1}(a_{d1}/b_{d1})$ (33)

And the supply power factor is:

$$Pf = (I_{df}/I_{dsrms})\cos\theta \quad (34)$$

Whereas the supply current distortion factor is:

$$Df = I_{df} / I_{dsrms} \quad (35)$$

The developed motor power is given by:

$$P_{motor} = K_{af} N I_{motorrms}^2 \quad (36)$$

and the motor torque is obtained from:

$$T_{motor} = K_{af} I_{motorrms}^2$$

3. System Performance

A computer program has been developed (based on the equations derived in section 2) to study the system performance. The following data of the load-combination parameters are used:

Motor: Ra1 =0.15 Ω. La1 =0.02 H. Kaf =0.03 H. Kres =0.075 V/rad/s.
Passive load: R2=1.0 Ω. L2=0.012 H.

and the rms value of the supply voltage is 120.0 volts.

3.1 Computer Results

3.1.1 Current Waveforms:

The waveforms of the converter, motor, and passive load currents are obtained using equations (3), (4) and (7) in the continuous mode and equations (18), (19), (21), (24), and (25) in the discontinuous mode. These waveforms are shown in figure 2 and figure 3 for continuous mode and in figure 4 for discontinuous mode.

3.1.2 Critical Firing Angle:

According to equation (15), the variation of the critical firing angle αc, with respect to the motor speed N, is shown in figure 5. It is noted that the critical firing angle αc, decreases in a non-linear fashion as the motor speed is increased.

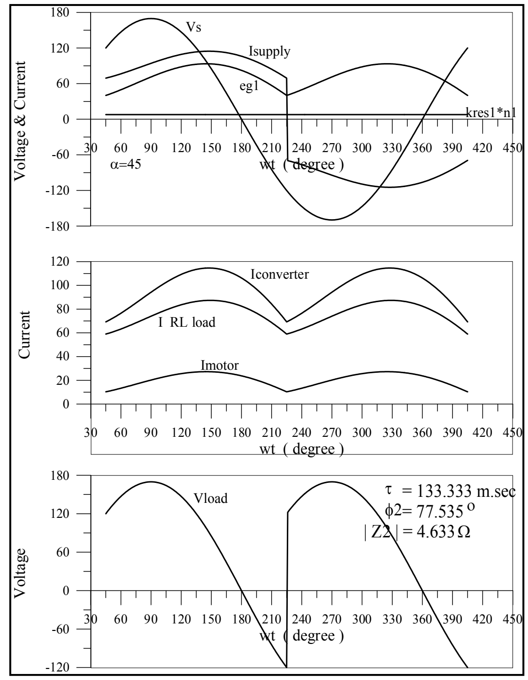

Figure 2. Current and voltage waveforms in the continuous converter current mode of operation for N=1000 rpm and α = 45°.

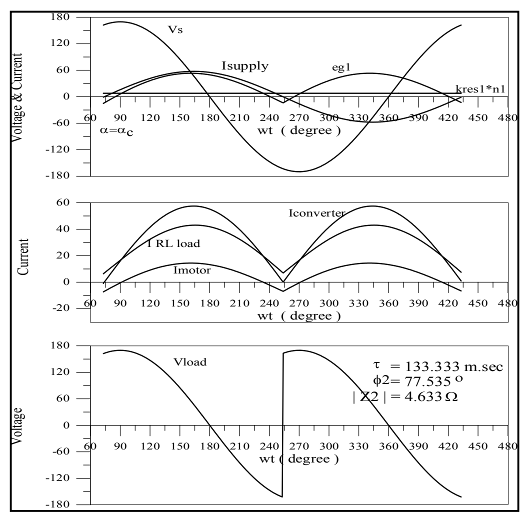

Figure 3. Current and voltage waveforms in the continuous converter current mode of operation for N=1000rpm and α = αc =73.922°.

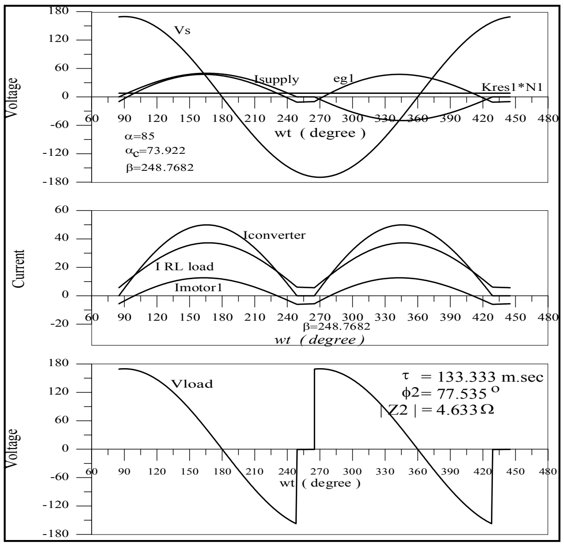

Figure 4. Current and voltage waveforms in the discontinuous converter current mode of operation for N=1000rpm and α=85°.

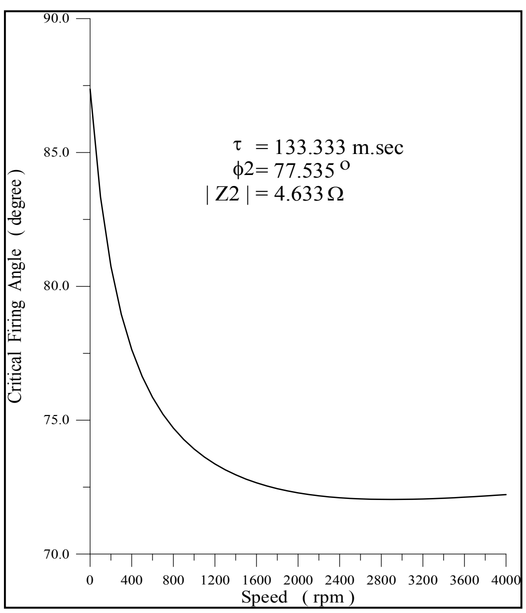

Figure 5. Critical firing angle versus motor speed

3.1.3 Motor Performance Parameters for Constant- HP Operation:

Series motors are normally used for constant-horsepower applications (Masilamani Muruganadam and Muthusamy Madheswaran,2013) and (Muruganadam M and Madheswaran M, 2012). However, the torque-speed curves for a particular firing angle do not conform to constant power characteristics. If the motor is required to operate at a constant power level, the firing angle has to be adjusted accordingly (Sen P C,1981).

Figure 6 shows the variation of firing angle α, with respect to the motor speed N, for different values of horsepower level, Hp. It is seen that α decreases as N, or the Hp, is increased

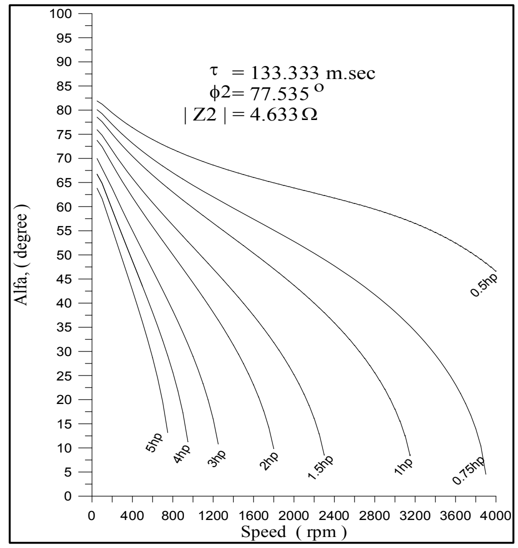

Figure 6. Firing angle versus motor speed at different values of horsepower level.

Different performance parameters are presented in figures 7-10. Figure 7 shows that the motor torque-speed, T-N, characteristics are drooping in nature. The system produces high torque at low speed and low torque at high speed which is typical for series dc motors (Stephen J Chapman,2012 and Fitzgerald, Kingsley A E C, Jr. and Umans S D,2003). Figure 8 shows that the supply power factor p.f. deteriorates with a decrease in motor speed N. Increasing the motor speed leads to higher motor branch resistance R1; thus leading to a higher power factor. Keeping the motor speed constant, the increase in the value of horsepower level, leads to a lower α, i.e. higher power factor as shown in Figure. 8. It is evident from figures 9 and 10 that, each of the supply current distortion factor Df, and motor current ripple factor Rf increases as the load horsepower is decreased provided that N is constant. The best distortion factor is obtained at α which is the closer to the critical value αc. For constant speed, as the value of Hp decreases, α is increased leading to a lower dc component of the motor current. Therefore Rf increases as shown in Figure 10 for constant N.

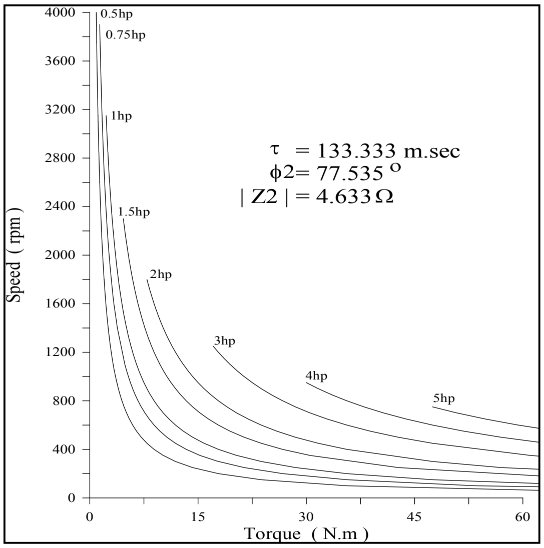

Figure 7. Torque-speed characteristics at different values of horsepower level.

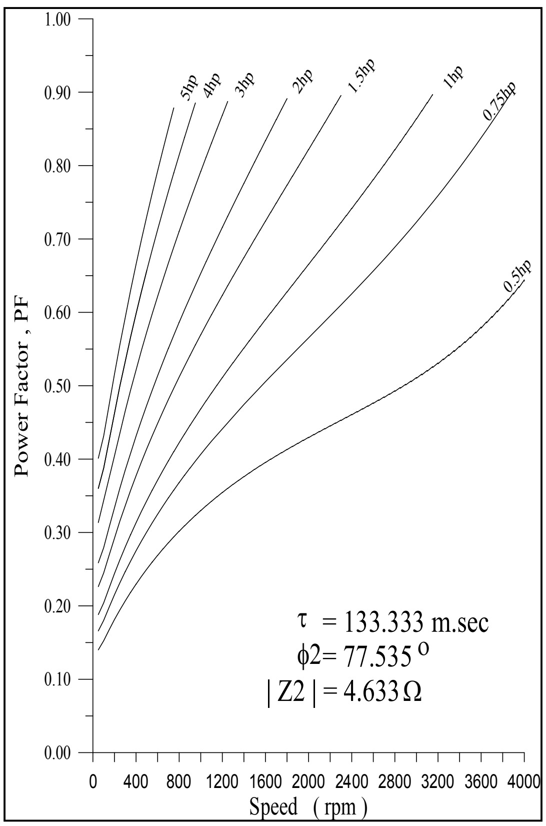

Figure 8. Supply power factor versus motor speed at different values of horsepower level.

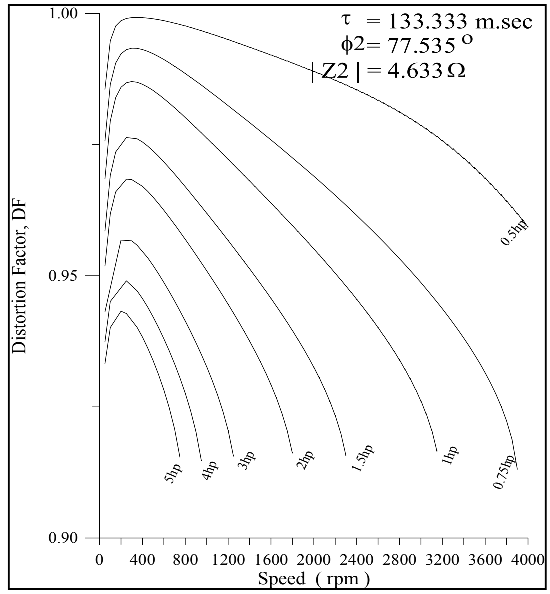

Figure 9. Supply current distortion factor versus motor speed at different values of horsepower level.

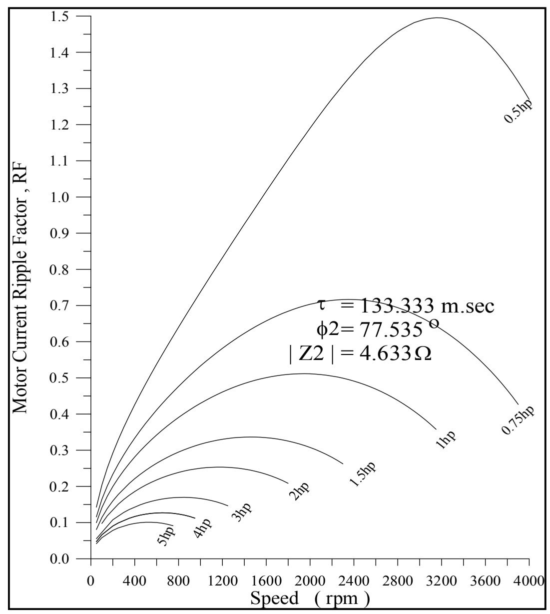

Figure 10. Motor current ripple factor versus motor speed at different values of horsepower level.

3.1.4 Motor Performance Parameters for Constant firing angle Operation:

Different performance parameters are shown in figures 11-14. Figure11 shows the T-N characteristics for different values of α. Dotted lines in the figure represent the regions of discontinuous converter current. As expected, the converter current is discontinuous at high values of α, high speed and low values of torque. Figure 12 shows that p.f. decreases as α, is increased. Increase of α leads to increase of the displacement angle of the fundamental component of the supply current which leads to a lower p.f. Figure13 shows that Df increases as α is increased for continuous converter current mode. Opposite conclusion is obtained for the discontinuous converter current mode. From figures 5 and 13, it is observed that, the best Df is obtained at α which is closest to αc. This was observed for constant Hp operation. Figure 14 shows that motor current Rf increases with increase either of α or N. Increasing α or N decreases the dc component of the motor current and this leads to high motor current Rf.

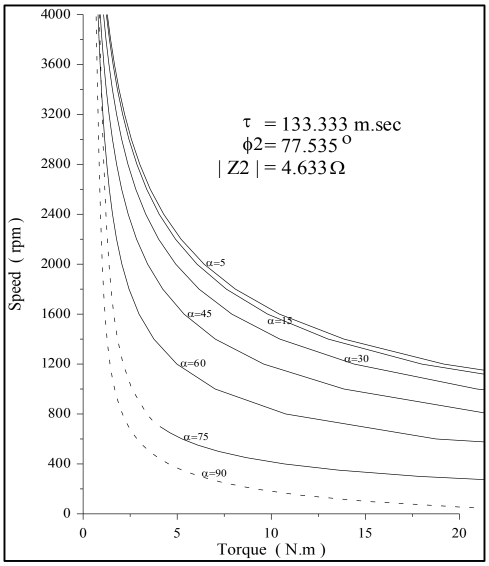

Figure11. Torque-speed characteristics at different values of firing angle.

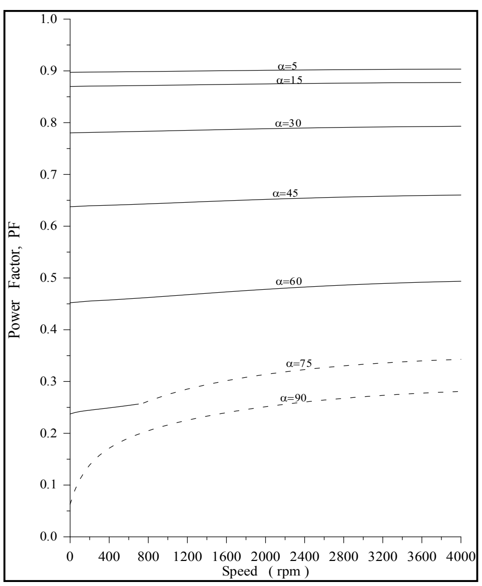

Figure 12. Supply power factor versus motor speed at different values of firing angle

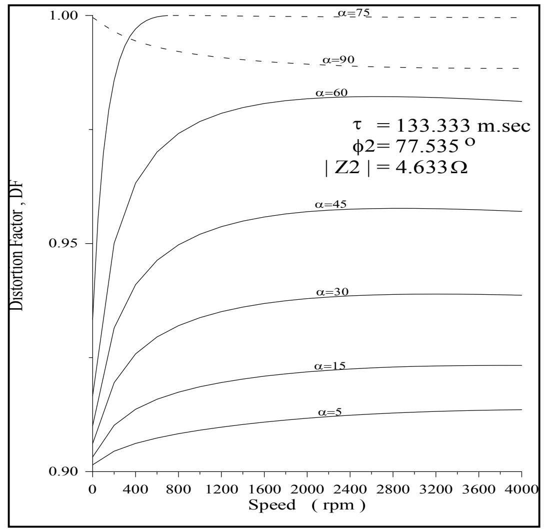

Figure 13. Supply current distortion factor versus motor speed at different values of firing angle

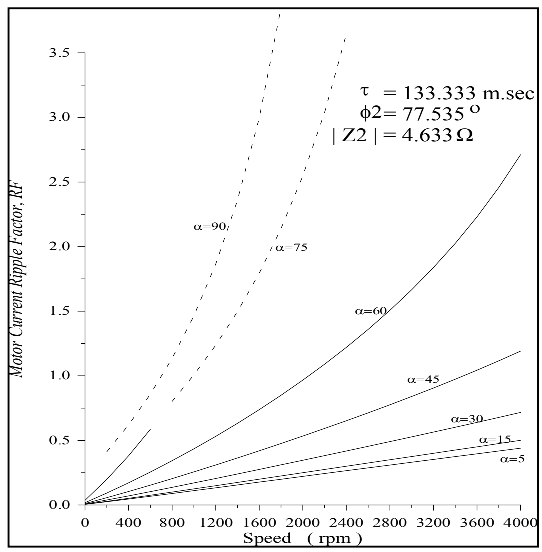

Figure 14. Motor current ripple factor versus motor speed at different values of firing angle.

3.1.5 Effect of load impedance.

3.1.5.1 ϕ_2 Variation.

The variation of α_c with respect to N for different values of passive load phase angle ϕ_2 is shown in Figure 15. As expected, when $|Z_2|$ and motor speed remain unaltered α_c increases as ϕ_2 is increased. T-N characteristics are shown in Figure 16. For the same speed high torque is obtained at low ϕ_2, keeping α constant. P.f. versus N is shown in Figure 17. P.f. is high for smaller ϕ_2, keeping α constant. Figure 18 shows the variation of motor current Rf versus N. Rf is low for smaller ϕ_2 , keeping α and motor speed constants.

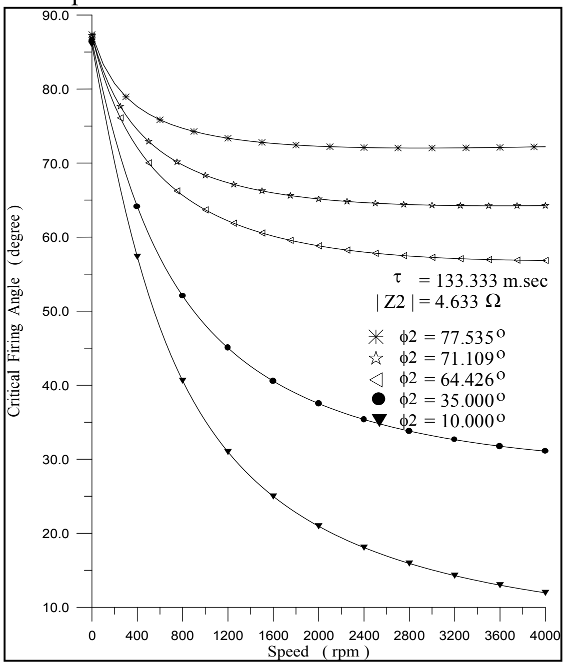

Figure 15. Critical firing angle versus motor speed at different values of passive load phase angle $\phi2$, keeping |Z2| unchanged.

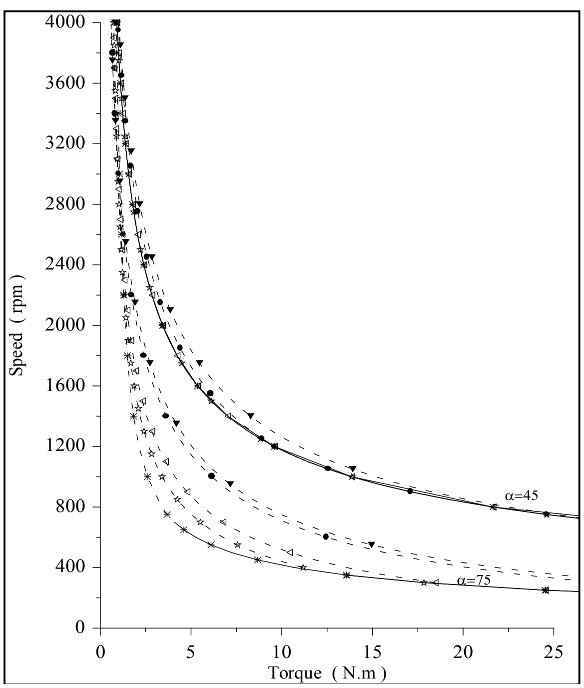

Figure 16. Torque-speed characteristics at different values of firing angle and for different values of passive load phase angle $\phi2$.

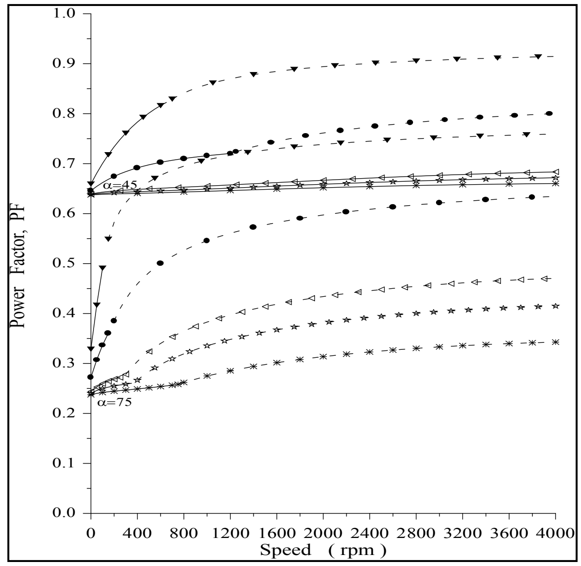

Figure 17. Supply power factor versus motor speed at different values of firing angle and for different values of passive load phase angle $\phi2$

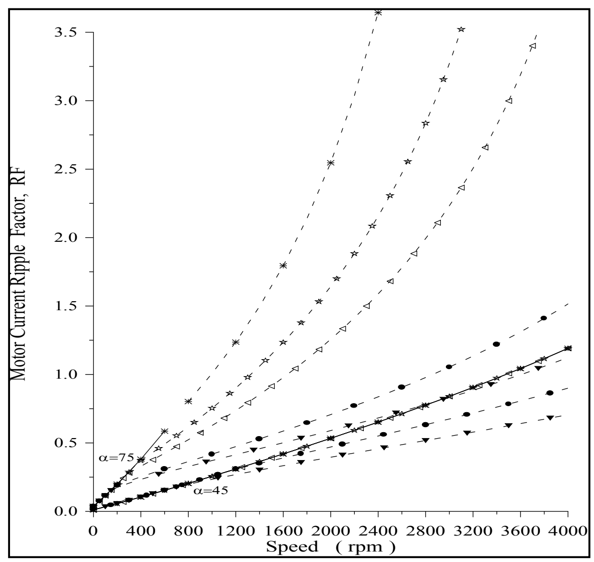

Figure 18. Motor current ripple factor versus motor speed at different values of firing angle and for different values of passive load phase angle $\phi2$.

3.1.5.2 |Z2| Variation.

The variation of αc with respect to N for different values of passive load impedance |Z2| are shown in figures 19 and 20 for $\phi2=55°$ and $\phi2=77.535$ °, respectively. The impedance |Z1b| is calculated at rated speed. It is noted that the curves intersect at a common αc where both loads have the same phase angle as αc. This confirms the fact that when $\phi1 = \phi2$, then αc equals both as could be shown from equation 15, assuming a negligible value of Kres is considered. At speeds lower than the intersection point speed Ni, the value of αc increases as |Z2| is increased. However, the situation is reveres for speeds higher than Ni. This is an interesting conclusion which is applicable under any situation as long as it is possible to have same phase angle for both loads. Figure 21 shows T-N characteristics. It is evident that in the continuous converter current mode of operation, the variation of |Z2| has no effect on the T-N characteristics. For the discontinuous converter current mode of operation and at speeds lower than Ni, the torque increases with the decrease of |Z2| for the same speed. The opposite is true for speeds above Ni. P.f. versus N is shown in Figure 22. It is clear that for the speed smaller than Ni, p.f. increases as |Z2| is decreased and the opposite is valid for speeds higher than Ni. The relationship between Df and N is presented in Figure 23. Again, the best distortion factor is obtained for α nearer to αc. The variation of motor current Rf versus N is shown in Figure 24. It is noted that, higher motor current Rf is obtained for higher |Z2| for speeds smaller than Ni. The opposite result is valid for speeds higher than Ni.

3.2 Experimental Results

In order to verify the accuracy and validity of the analysis presented an AC-DC full controlled converter has been assembled. A firing circuit has been designed and built to match the scheme of cosine control of the firing angle α.

The following load parameters are measured:

Motor:	Passive load:
Ra1=0.61Ω.	R2=3.83Ω.
La1=0.0053 H.	L2=0.043 H. (unsaturated)
Kaf=0.0099222 H.	
Kres=0.0247446 V/rad/s.	

and the rms value of the supply voltage is 120.0 volts.

The experimental oscillograms of il, i1 and i2 are shown in Figure 25 and Figure26 for continuous mode of operation at α=48 ° and at αc=55.64 ° respectively. The experimental oscillograms of these currents are shown in Figure 27 for discontinuous mode of operation at α=78.55 °. The same parameters of the loads connected to the assembled converter have been entered to the computer program developed to get the waveforms of the total load current and the branch currents at various firing angles. The theoretical waveforms of the branch currents i1 and i2 and the total load current il at firing angles of 48, 55.64 and 78.55 are shown in Figures 28, 29 and 30 respectively. Inspecting the theoretical and experimental results, it is evident that they are in good agreement. This confirms and verifies the validity and accuracy of the analysis developed in this paper.

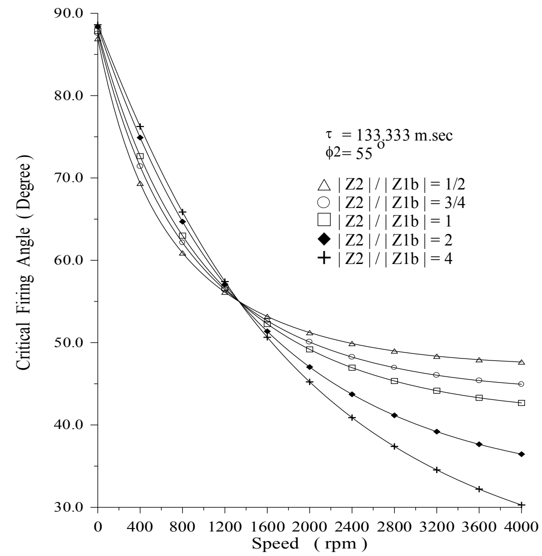

Figure 19. Critical firing angle versus motor speed for different values of passive load impedance |Z2| keeping ϕ2 =55°.

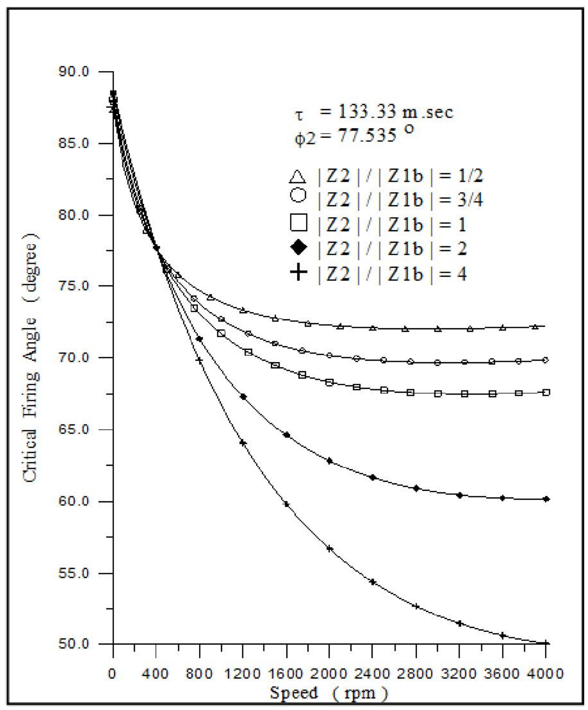

Figure 20. Critical firing angle versus motor speed for different values of passive load impedance |Z2| keeping ϕ2 =77.535°.

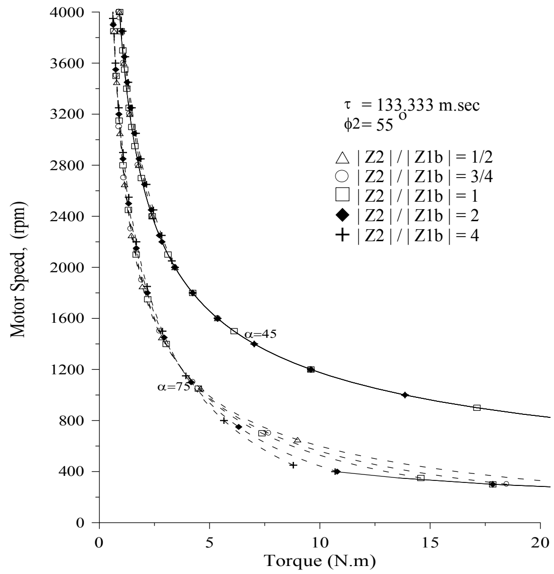

Figure 21. Torque-speed characteristics at different values of firing angle for different value of passive load impedance |Z2| keeping ϕ2 =55°.

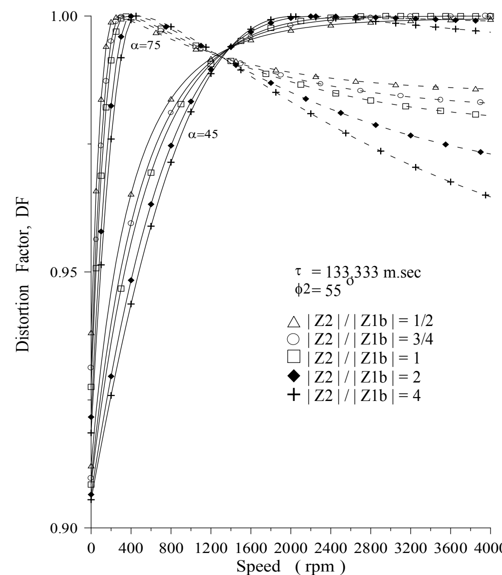

Figure 23. Supply current distortion factor versus motor speed at different values of firing angle for different value of passive load impedance |Z2| keeping ϕ2 =55°.

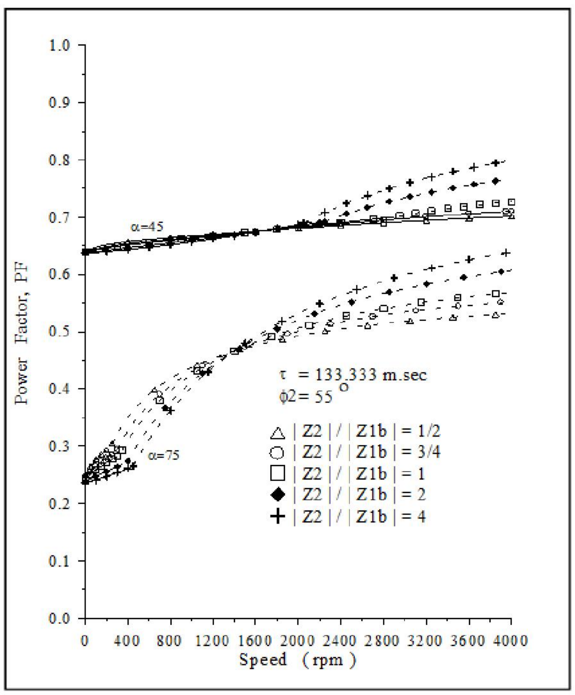

Figure 22. Supply power factor versus speed at different values of firing angle for different value of passive load impedance |Z2| keeping ϕ2 =55°.

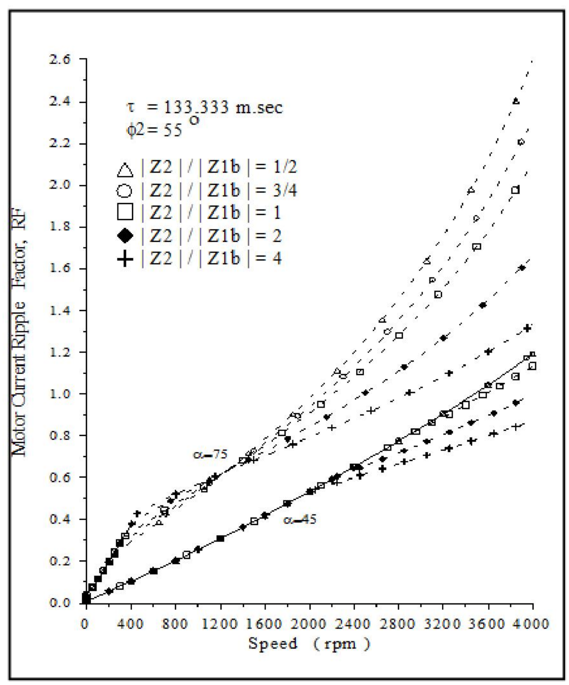

Figure 24. Motor current ripple factor versus motor speed at different values of firing angle for different value of passive load impedance |Z2| keeping ϕ2 =55°.

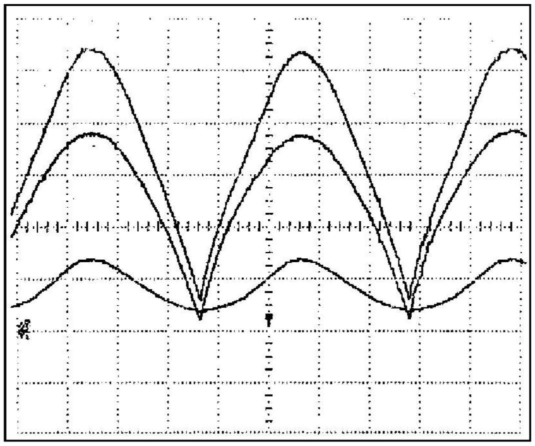

Continuous converter current mode

Figure 25. Oscillograms of the converter current, icl, motor current, ic1, and passive load current, ic2, at α = 48°, N=800 rpm (time scale = 2 m.sec./div, current scale = 20 amp/div).

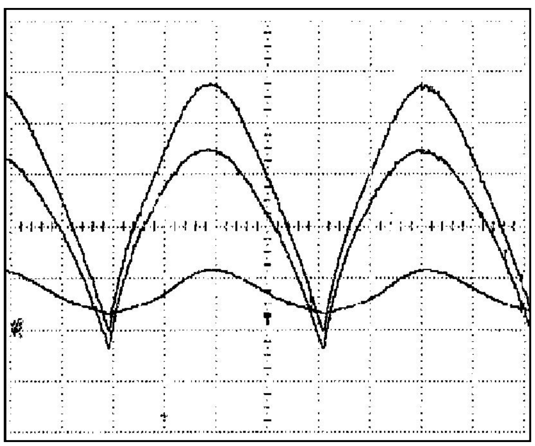

Figure 26. Oscillograms of the converter current, icl, motor current, ic1, and passive load current, ic2, at α = αc = 55.64°, N=800 rpm (time scale = 2 m.sec./div, current scale = 20 amp/div).

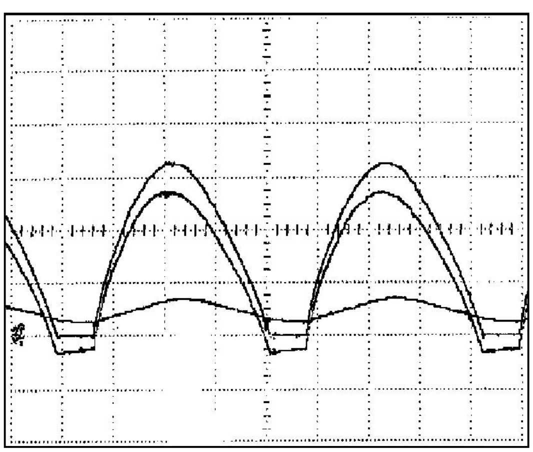

Discontinuous converter current mode

Figure 27. Oscillograms of the converter current, idl, motor current id1, and passive load current, id2, at α = 78.55°, N=800 rpm (time scale = 2 m.sec./div, current scale = 20 amp/div).

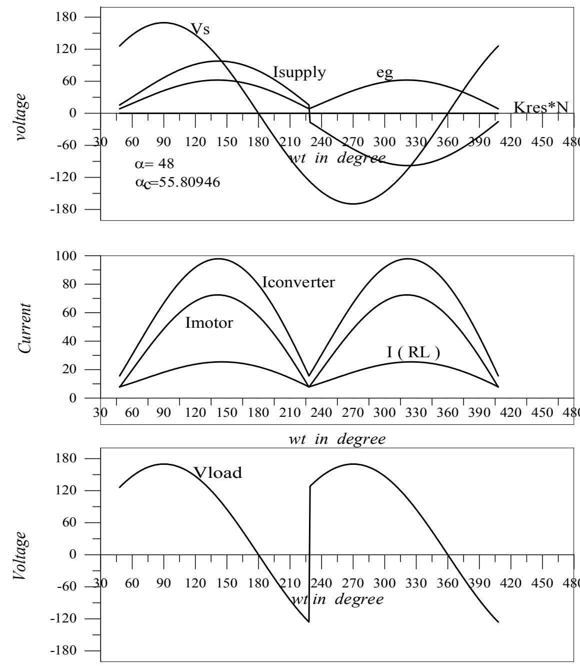

Figure 28. Current and voltage waveforms in the continuous converter current mode of operation for N=800 rpm and α= 48°.

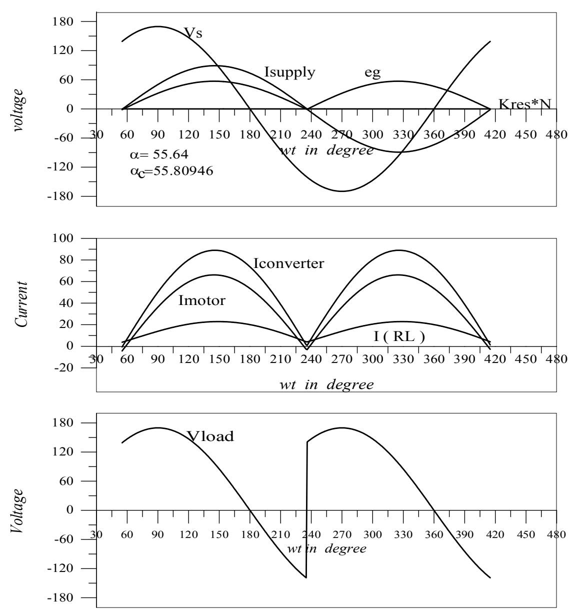

Figure 29. Current and voltage waveforms for N=800 rpm and α = αc = 55.64°.

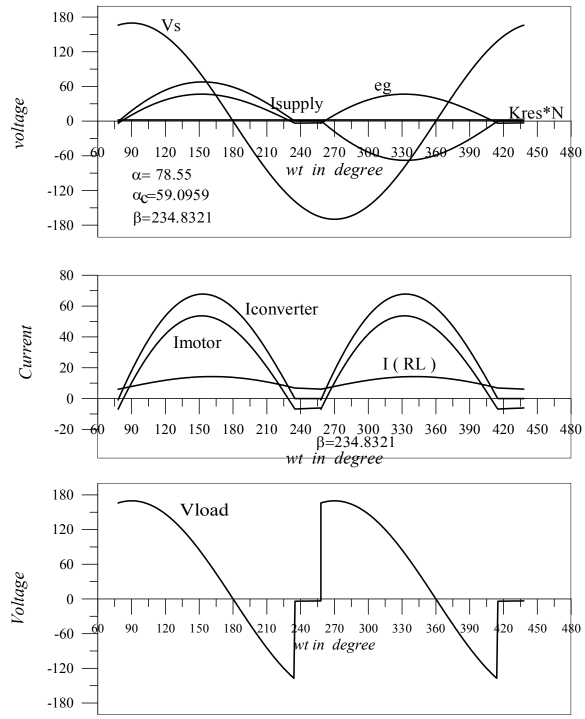

Figure 30 Current and voltage waveforms in the discontinuous converter current mode of operation for N=800 rpm and α = 78.55°.

4. Conclusions

In this paper, an ac-dc full-controlled converter supplying a series dc motor parallel with an inductive R-L load has been investigated. The steady-state analysis of the system has been derived analytically for each of the two modes of operation (continuous and discontinuous converter current). In each mode, the developed expressions are: converter, motor, passive load currents, motor current ripple factor, torque-speed characteristic, input power factor, and supply current distortion factor. Also the critical firing angle has been derived and investigated. The effect of variation of the passive load phase angle and impedance has been studied. The theoretical and experimental results are compared to check model effectiveness. In view of the analysis and results presented in this paper, the following conclusions have been inferred:

4.1 Critical firing angle αc:

The critical firing angle αc increases as the motor speed N is decreased and as the passive load phase angle ϕ2 is increased. At speeds lower than Ni (where both loads have the same phase angle), αc increases as the passive load impedance |Z2| is increased. However, the situation is reverse for speeds higher than Ni. When ϕ1 =ϕ2 =ϕ, then α_c =ϕ, ignoring the effect of K_{res} .

4.2 Supply Current Df:

The best distortion factor Df is obtained at α which is the closer to the critical value αc.

4.3 Constant Passive Load Impedance:

(a)Constant HP operation:

During this situation, α decreases and the input p.f. increases as the motor speed N is increased.

b) Constant Speed N operation:

The increase in the value of horsepower level HP leads to a lower α, higher p.f, and a lower Df and motor current Rf. Decreasing the firing angle α increases the input p.f. and decreases the motor current Rf.

c) Constant Firing Angle α operation:

The increase in the motor speed N leads to decrease of the horsepower level Hp, small variation of p.f, and higher Rf.

4.4 ϕ2 Variation:

Keeping α, N, and |Z2| Constants and for the continuous converter current mode of operation, the variation of ϕ2 has no effect on the T-N characteristics and Rf. In the discontinuous mode of operation, high torque is obtained at low ϕ2 and high Rf is obtained at high ϕ2. The p.f. increases for both mode as ϕ2 is decreased.

4.5 |Z2| Variation:

Keeping α, N, and ϕ2 Constants it is evident that, the variation of |Z2| has no effect on the T-N characteristics and Rf in the continuous converter current mode of operation. For the discontinuous mode of operation and at speeds lower than Ni, the torque increases, Rf decreases with the decrease of |Z2|, and p.f. increases for both mode as |Z2| is decreased. The opposite is valid for speeds higher than Ni.

References

1. Masilamani Muruganadam and Muthusamy Madheswaran. Stability analysis and Implementation of Chopper fed DC Series Motor with Hyprid PID-ANN Controller. International Journal of Control Automation and Systems, 2013;11(5): 966-975.
2. Muruganadam M and Madheswaran M. Experimental verification of Chopper Fed DC Series Motor with ANN Controller. Higher Education Press and Springer-Verlag Berlin Heidelberge, 2012.
3. Hart D H. power Electronics. 1st ed., McGraw Hill, 2011.

4. Rashid M H. power Electonics: Circuits, Devices, and applications. ,pearson prentice-Hall,2004.
5. Singh M D, khanchendani K B. power electronics. Tata McGraw Hill, 2003
6. Sen P C. Thyristor DC Drives. John Wiley, 1981.
7. Stephen J. chapman. Electric Machinery Fundamentals. 5th ed, McGraw-Hill, 2012.
8. Fitzgerald, Kingsley A E C, Jr., and Umans S D. Electric Machinery. 6th ed. McGraw-Hill,2003.
9. Yung-Chung Li. Steady-State Analysis of a Two-Branch Resistance-Inductance Parallel Circuit Controlled By a Forced-Commutation Bidirectional AC Switch. IEEE Transactions on Industrial Electronics and Control Instrumentation, Nov. 1978.
10. AL-Johani A. H. Analysis of an AC-DC Converter Supplying Two Parallel Inductive Loads. Master Thesis, KAU, 1987.
11. Sen P C and Dorodla S R. Solid-State Series Motor Drive. IEEE Transactions on Industrial Electronics and control Instrumentation, May 1975.
12. Sen P C and Dorodla S R. Evaluation of Control Schemes for Thyristor-Controlled DC Motors. IEEE Transactions on Industrial Electronics and Control Instrumentation, August 1978.
13. Arthur W. Kelley and William F. Yadusky. Phase-Controlled Rectifier Line-Current Harmonics and Power Factor as a Function of Firing Angle and Output Filter Inductance. IEEE Transaction on Industrial Electronics, 1990: 588-597.
14. Sen P C. Electric Motot Drives and Control-Past, Present, and future. IEEE Transactions on Industrial Electronics, 1990.
15. AL-Subaie O. T. Analysis of a Controlled Rectifier Supplying Two Motor Loads. Master Thesis, KAU, May 1999.
16. Al-Turki Y, Al-Hindawi M M and Al-Subaie O T. Analysis of an AC-DC Full Converter Supplying Separately Excited DC Motor Parallel with an Inductive R-L Load. UPEC 2000,6-8 September 2000, Belfast, Northern.
17. Al-Turki Y A, Al-Hindawi M M and Al-Subai O T. Analysis of an AC-DC Full-controlled Converter Supplying Separately Excited DC Motor Parallel With Series DC Motor Loads JKAU, Eng. Sci. , 2001;13(2): 43-71.
18. Al-Hindawi M M, Al-Turki Y A and Maghrabi M. Analysis of an AC-DC Simi-Converter Supplying Series DC Motor Parallel With An Inductive R-L Load. JES, Assuit University, 2006;33(1) : 47-67.
19. Al-Hindawi M M, Al-Turki Y A and Al-Subaie O T. Analysis Of An AC-DC Full-controlled Converter Supplying Two DC Series Motor Loads. The Arabian Journal For Science And Engineering , 2000; 25(1B): 31-46.

Appendix

Continuous mode.

The average value of the motor current is obtained from: $I_{c1av} = (1/\pi)\int_{\alpha}^{\pi+\alpha} i_{c1} d\omega t$ and is given by:

$$I_{c1av} = 2\sqrt{2}(V/\pi Z_1)\cos(\alpha-\phi_1) + (K_{c1}Q_1/\pi)(1-e^{(-\pi/Q_1)}) - (K_{res}N/R_1)[1-(Q_1/\pi)(1-e^{(-\pi/Q_1)})] \quad \text{(A-1)}$$

The r.m.s value of the motor current is obtained from:

$I_{c1rms} = \sqrt{(1/\pi)\int_{\alpha}^{\pi+\alpha} i_{c1}^2 d\omega t}$ and is given by:

$$I_{c1rms} = [(V^2/Z_1^2) + (K_{c1}+(K_{res}N/R_1))(2\sqrt{2}VQ_1^2/(\pi Z_1(1+Q_1^2))) [(1/Q_1)\sin(\alpha-\phi_1)+\cos(\alpha-\phi_1)](1+e^{(-\pi/Q_1)}) - (4\sqrt{2}VK_{res}N/\pi Z_1R_1) \cos(\alpha-\phi_1) + (Q_1/2\pi)(K_{c1}+(K_{res}N/R_1))^2(1-e^{(-2\pi/Q_1)}) - (2Q_1K_{res}N/\pi R_1)(K_{c1}+(K_{res}N/R_1))(1-e^{(-\pi/Q_1)}) + (K_{res}N/R_1)^2]^{1/2} \quad \text{(A-2)}$$

The average value of the ic2 is:

$$I_{c2av} = 2\sqrt{2}(V/\pi Z_2)\cos(\alpha-\phi_2) + (K_{c2}Q_2/\pi)(1-e^{(-\pi/Q_2)}) \quad \text{(A-3)}$$

The rms value of the ic2 is:

$$I_{c2rms} = [(V^2/Z_2^2) + K_{c2}(2\sqrt{2}VQ_2^2/(\pi Z_2(1+Q_2^2))) [(1/Q_2)\sin(\alpha-\phi_2)+\cos(\alpha-\phi_2)](1+e^{(-\pi/Q_2)}) + (Q_2/2\pi)K_{c2}^2(1-e^{(-2\pi/Q_2)})]^{1/2} \quad \text{(A-4)}$$

ac1 and bc1 are the amplitudes of the cosine and sine fundamental components of ics respectively and are given by: $a_{c1} = (1/\pi)\int_{\alpha}^{2\pi+\alpha} i_{cs}\cos\omega t\, d\omega t$ and is obtained from:

$$a_{c1} = -(\sqrt{2}V/Z_1)\sin\phi_1 + (2Q_1^2/(1+Q_1^2)\pi)(K_{c1}+(K_{res}N/R_1)) ((1/Q_1)\cos\alpha-\sin\alpha)(1+e^{(-\pi/Q_1)}) + (4K_{res}N/\pi R_1)\sin\alpha - (\sqrt{2}V/Z_2)\sin\phi_2 + (2Q_2^2/(1+Q_2^2)\pi)(K_{c2}) ((1/Q_2)\cos\alpha-\sin\alpha)(1+e^{(-\pi/Q_2)}) \quad \text{(A-5)}$$

And $b_{c1} = (1/\pi)\int_{\alpha}^{2\pi+\alpha} i_{cs}\sin\omega t\, d\omega t$, and is obtained from:

$$b_{c1} = (\sqrt{2}V/Z_1)\cos\phi_1 + (2Q_1^2/(1+Q_1^2)\pi)(K_{c1}+(K_{res}N/R_1))((1/Q_1)\sin\alpha+\cos\alpha)(1+e^{(-\pi/Q_1)}) - (4K_{res}N/\pi R_1)\cos\alpha + (\sqrt{2}V/Z_2)\cos\phi_2 + (2Q_2^2/(1+Q_2^2)\pi)(K_{c2})((1/Q_2)\sin\alpha+\cos\alpha)(1+e^{(-\pi/Q_2)}) \quad \text{(A-6)}$$

Discontinuous mode.

The average value of the motor current is given by: $I_{d1av} = (1/\pi)\int_{\alpha}^{\pi+\alpha} i_{d1} d\omega t$. Therefore:

$$I_{d1av} = (\sqrt{2}V/Z_1\pi)[\cos(\alpha-\phi_1)-\cos(\beta-\phi_1)] + (Q_1/\pi)(K_{d1}+(K_{res}N/R_1))(1-e^{(-(\beta-\alpha)/Q_1)}) + (K_{res}N/R_1)((\alpha-\beta)/\pi) + ((-K_{res}N)/(R_1+R_2))((\pi+\alpha-\beta)/\pi) + (Q/\pi)(((-K_{res}N)/(R_1+R_2)) - I'_{d1})(e^{(-(\pi+\alpha-\beta)/Q)}-1) \quad \text{(A-7)}$$

The r.m.s value of the motor current is found to be: $I_{d1rms} = \sqrt{(1/\pi)\int_{\alpha}^{\pi+\alpha} i_{d1}^2 d\omega t}$. Therefore:

$$I_{d1rms} = \{(2V^2/\pi Z_1^2)[(\beta-\alpha)/2+[\sin2(\alpha-\phi_1)-\sin2(\beta-\phi_1)]/4] + (2\sqrt{2}V/\pi Z_1)(K_{res}N/R_1)[\cos(\beta-\phi_1)-\cos(\alpha-\phi_1)] + (2\sqrt{2}V/\pi Z_1)(Q_1^2/(1+Q_1^2))(K_{d1}+(K_{res}N/R_1))[e^{(-(\beta-\alpha)/Q_1)}(-(1/Q_1)\sin(\beta-\phi_1)-\cos(\beta-\phi_1))+((1/Q_1)\sin(\alpha-\phi_1)+\cos(\alpha-\phi_1))] - (Q_1/2\pi)(K_{d1}+(K_{res}N/R_1))^2(e^{(-2(\beta-\alpha)/Q_1)}-1) + (Q_1/\pi)(2K_{d1}(K_{res}N/R_1)+2(K_{res}N/R_1)^2)(\,^{(-(\beta-\alpha)/Q_1)}-1) + (K_{res}N/R_1)^2(\beta-\alpha)/\pi + ((-K_{res}N)/(R_1+R_2))^2((\pi+\alpha-\beta)/\pi) + (2Q/\pi)[((-K_{res}N)/(R_1+R_2))^2 - I'_{d1}(-K_{res}N/(R_1+R_2))](e^{(-(\pi+\alpha-\beta)/Q)}-1) - (Q/2\pi)((-K_{res}N/(R_1+R_2))-I'_{d1})^2(e^{(-2(\pi+\alpha-\beta)/Q)}-1)\}^{1/2}$$

(A-8)

The average value of the passive load current is:

$$I_{d2av} = (\sqrt{2}V/Z_2\pi)[\cos(\alpha-\phi_2)-\cos(\beta-\phi_2)] + (Q_2/\pi)K_{d2}(1-e^{(-(\beta-\alpha)/Q_2)}) + ((K_{res}N)/(R_1+R_2))((\pi+\alpha-\beta)/\pi) + (Q/\pi)(((K_{res}N)/(R_1+R_2)) - I'_{d2})(e^{(-(\pi+\alpha-\beta)/Q)}-1)$$

(A-9)

The r.m.s value of the passive load current is:

$$I_{d2rms} = \{(2V^2/\pi Z_2^2)[(\beta-\alpha)/2+[\sin2(\alpha-\phi_2)-\sin2(\beta-\phi_2)]/4] + (2\sqrt{2}V/\pi Z_2)(Q_2^2/(1+Q_2^2))(K_{d2})[e^{(-(\beta-\alpha)/Q_2)}(-(1/Q_2)\sin(\beta-\phi_2)-\cos(\beta-\phi_2))+((1/Q_2)\sin(\alpha-\phi_2)+\cos(\alpha-\phi_2))] - (Q_2/2\pi)(K_{d2})^2(e^{(-2(\beta-\alpha)/Q_2)}-1) + ((K_{res}N)/(R_1+R_2))^2((\pi+\alpha-\beta)/\pi) + (2Q/\pi)[((K_{res}N)/(R_1+R_2))^2 - I'_{d2}((K_{res}N)/(R_1+R_2))](e^{(-(\pi+\alpha-\beta)/Q)}-1) - (Q/2\pi)(((K_{res}N)/(R_1+R_2))-I'_{d2})^2(e^{(-2(\pi+\alpha-\beta)/Q)}-1)\}^{1/2}$$

(A-10)

The r.m.s value of the supply current is obtained from:

$$I_{dsrms} = \sqrt{(1/\pi)\int_{\alpha}^{\beta} i_{ds}^2 d\omega t}$$

Thus:

$$I_{dsrms} = \sqrt{(1/\pi)\int_{\alpha}^{\beta} i_{d1}^2 d\omega t + (1/\pi)\int_{\alpha}^{\beta} i_{d2}^2 d\omega t + (1/\pi)\int_{\alpha}^{\beta} 2 i_{d1} i_{d2} d\omega t}$$

(A-11)

Then r.m.s value of the supply current is found to be:

$$I_{dsrms} = \{(2V^2/\pi Z_1^2)[(\beta-\alpha)/2+[\sin2(\alpha-\phi_1)-\sin2(\beta-\phi_1)]/4] + (2\sqrt{2}V/\pi Z_1)(K_{res}N/R_1)[\cos(\beta-\phi_1)-\cos(\alpha-\phi_1)] + (2\sqrt{2}V/\pi Z_1)(Q_1^2/(1+Q_1^2))(K_{d1}+(K_{res}N/R_1))[e^{(-(\beta-\alpha)/Q_1)}(-(1/Q_1)\sin(\beta-\phi_1)-\cos(\beta-\phi_1))+((1/Q_1)\sin(\alpha-\phi_1)+\cos(\alpha-\phi_1))] - (Q_1/2\pi)(K_{d1}+(K_{res}N/R_1))^2(e^{(-2(\beta-\alpha)/Q_1)}-1) + (Q_1/\pi)(2K_{d1}(K_{res}N/R_1)+2(K_{res}N/R_1)^2)(e^{(-(\beta-\alpha)/Q_1)}-1) + (K_{res}N/R_1)^2(\beta-\alpha)/\pi + (2V^2/\pi Z_2^2)[(\beta-\alpha)/2+[\sin2(\alpha-\phi_2)-\sin2(\beta-\phi_2)]/4] + (2\sqrt{2}V/\pi Z_2)(Q_2^2/(1+Q_2^2))(K_{d2})[e^{(-(\beta-\alpha)/Q_2)}(-(1/Q_2)\sin(\beta-\phi_2)-\cos(\beta-\phi_2))+((1/Q_2)\sin(\alpha-\phi_2)+\cos(\alpha-\phi_2))] - (Q_2/2\pi)(K_{d2})^2(e^{(-2(\beta-\alpha)/Q_2)}-1) + (2V^2/\pi Z_1Z_2)\cos(\phi_2-\phi_1)(\beta-\alpha) - (V^2/\pi Z_1Z_2)[\sin(2\beta-\phi_2-\phi_1)-\sin(2\alpha-\phi_2-\phi_1)] + (2\sqrt{2}V/\pi Z_2)(K_{res}N/R_1)[\cos(\beta-\phi_2)-\cos(\alpha-\phi_2)] + (2\sqrt{2}V/\pi Z_2)(Q_1^2/(1+Q_1^2))(K_{d1}+(K_{res}N/R_1))[e^{(-(\beta-\alpha)/Q_1)}(-(1/Q_1)\sin(\beta-\phi_2)-\cos(\beta-\phi_2))+((1/Q_1)\sin(\alpha-\phi_2)+\cos(\alpha-\phi_2))] + (2\sqrt{2}V/\pi Z_1)(Q_2^2/(1+Q_2^2))(K_{d2})[e^{(-(\beta-\alpha)/Q_2)}(-(1/Q_2)\sin(\beta-\phi_1)-\cos(\beta-\phi_1))+((1/Q_2)\sin(\alpha-\phi_1)+\cos(\alpha-\phi_1))] + (2Q_1Q_2/\pi(Q_1+Q_2))(K_{d1}+(K_{res}N/R_1))(K_{d2})(1-e^{(-(Q_1+Q_2)(\beta-\alpha)/Q_1Q_2)}) + (2Q_2/\pi)(K_{res}N/R_1)(K_{d2})(e^{(-(\beta-\alpha)/Q_2)}-1)\}^{1/2}$$

(A-12)

And, ad1 and bd1 are the amplitudes of the cosine and sine fundamental components of ids respectively and are given by:

$$a_{d1} = (\sqrt{2}V / 2\pi Z_1)[\cos(2\alpha - \phi_1) - \cos(2\beta - \phi_1) - 2(\beta - \alpha)\sin\phi_1] +$$
$$2(Q_1^2 /(\pi(1 + Q_1^2)))(K_{d1} + (K_{res}N / R_1))[e^{(-(\beta-\alpha)/Q_1)}(-(1/Q_1)$$
$$\cos\beta + \sin\beta) + ((1/Q_1)\cos\alpha - \sin\alpha)] - (2K_{res}N / \pi R_1))$$
$$(\sin\beta - \sin\alpha) + (\sqrt{2}V / 2\pi Z_2)[\cos(2\alpha - \phi_2) - \cos(2\beta - \phi_2) -$$
$$2(\beta - \alpha)\sin\phi_2] + 2(Q_2^2 /(\pi(1 + Q_2^2)))(K_{d2})[e^{(-(\beta-\alpha)/Q_2)}$$
$$(-(1/Q_2)\cos\beta + \sin\beta) + ((1/Q_2)\cos\alpha - \sin\alpha)], and$$

(A-13)

$$b_{d1} = (\sqrt{2}V / 2\pi Z_1)[\sin(2\alpha - \phi_1) - \sin(2\beta - \phi_1) + 2(\beta - \alpha)\cos\phi_1] +$$
$$2(Q_1^2 /(\pi(1 + Q_1^2)))(K_{d1} + (K_{res}N / R_1))[e^{(-(\beta-\alpha)/Q_1)}(-(1/Q_1)$$
$$\sin\beta - \cos\beta) + ((1/Q_1)\sin\alpha + \cos\alpha)] + (2K_{res}N / \pi R_1))$$
$$(\cos\beta - \cos\alpha) + (\sqrt{2}V / 2\pi Z_2)[\sin(2\alpha - \phi_2) - \sin(2\beta - \phi_2) +$$
$$2(\beta - \alpha)\cos\phi_2] + 2(Q_2^2 /(\pi(1 + Q_2^2)))(K_{d2})[e^{(-(\beta-\alpha)/Q_2)}$$
$$(-(1/Q_2)\sin\beta - \cos\beta) + ((1/Q_2)\sin\alpha + \cos\alpha)]$$

(A-14).

5/16/2014